PCCP

Accepted Manuscript

ROYAL SOCIETY OF CHEMISTRY

www.rsc.org/pccp

Effect of multilayer structure, stacking order and external electric field on electrical properties of few-layer boron-phosphide

Xianping Chen,[*ab†] Chunjian Tan,[a†] Qun Yang,[a] Ruishen Meng,[a] Qiuhua Liang,[b] Junke Jiang,[b] Xiang Sun,[b] D.Q. Yang,[a] and Tianling Ren[*c]

[a]Faculty of Electromechanical Engineering, Guilin University of Electronic Technology, 541004 Guilin, China. xianpingchen1979@126.com

[b]Key Laboratory of Optoelectronic Technology & Systems, Education Ministry of China, Chongqing University, Chongqing 400044, China

[c]Institute of Microelectronics, Tsinghua University, 100084 Beijing, China. RenTL@tsinghua.edu.cn

†These authors contributed equally to this work.

Abstract

Development of nanoelectronics requires two-dimensional (2D) systems with both direct-bandgap and tunable electronic properties as they act in response to external electric field (E-field). Here, we present a detailed theoretical investigation to predict the effect of atomic structure, stacking order and external electric field on the electrical properties of few-layer boron-phosphide (BP). We demonstrate that the splitting of bands and bandgap of BP depends on the number of layer and the stacking order. The values for bandgap show a monotonically decreasing relationship with the increased layer number. We also show that AB-stacking BP has a direct-bandgap, while ABA-stacking BP has an indirect-bandgap when the number of layer n > 2. In addition, for bilayer and trilayer, the bandgap will increase (decrease) as the electric field increasing along positive direction of external electric field (E-field) (negative direction). In the case of four-layer BP, the bandgap exhibits a nonlinearly decreasing behavior as the electric field increase is independent of the electric field direction. The tunable mechanism of bandgap can be attributed to a giant Stark effect. Interestingly, the investigation also shows that a semiconductor-to-metal transition may occur for the four-layer

case or more layers beyond critical electric field. Our findings may inspire more efforts in fabricating new nanoelectronics devices based on few-layer BP.

1. Introduction

Nowadays, two-dimensional (2D) materials represented by graphene have drawn lots of attention and been extensively studied in electronic applications due to their various intriguing properties such as extremely high mobility, excellent optical and thermal properties.[1-3] A good candidate material for electronics applications often requires a moderate electronic bandgap, a reasonably high carrier mobility, and excellent electrode-channel contacts.[4] However, most of current 2D materials including graphene, silicone, germanene, and other analogues, are gapless.[5-7] Extensive efforts following a wide variety of approaches have greatly contributed to search 2D crystal semiconductors with a direct-bandgap or to solve the issue of opening a gap in different 2D nanostructures. For instance, a new category of layered direct-bandgap semiconductor, few-layer black phosphorus,[8] has been theoretically discovered; and its electrical properties can be tuned regularly by the stacking order[9,10] or by applying in-plane strain and external electric field (E-field).[8,11-13] Meanwhile, the few-layer phosphorene with high anisotropy has also been successfully isolated from bulk black phosphorus.[4,14,15] Moreover, field-effect transistors (FET) based on few-layer black phosphorus crystals with thickness down to a few nanometers have been successfully fabricated, and this new nanodevice exhibits a good device performance with a high on/off ratio of 10^4.[16,17] Although phosphorene possesses the merits of both direct-bandgap and high hole mobility, the puckered lattice limits its wider application in electronics due to the incapability of controlling the movement of charge carrier within 2D range. Therefore, it is necessary to continue the exploration of new 2D planar materials which are semiconductors with a direct-bandgap and preferably has the potential in electronic applications.

The successful prediction of monolayer honeycomb structures of group-IV elements and III-V binary compounds has awakened an enormous interest in these 2D material

systems[18], and the monolayer boron-phosphide (BP) is especially attractive due to the flat 2D honeycomb lattice similar to graphene. The monolayer BP has an in-plane Young's modulus and Poisson's ratio of 135.6 N m^{-1} and 0.27, respectively, which suggests that the mechanical stability is almost the same with MoS_2 and less stiffer than both graphene and monolayer BN.[18,19] Unlike graphene, silicone, and germanene, the monolayer BP possesses a direct-bandgap, which may make it a very promising candidate material in the next generation of nanoelectronic and optoelectronic applications. Many previous studies[4,8,12,15,20] have shown that few-layer structure not only can maintain the inherent material properties of monolayer 2D materials, but also is more likely to be processed into micro/nanoelectronic devices. Motivated by this, it will be very worthy to investigate the electronic properties of few-layer BP.

According to the interior (the stacking order and layer number) and exterior (E-field) factors, we present the theoretical investigation of the structural and electronic properties of few-layer BP, particularly its tunability, by using first-principles calculations based on the density functional theory (DFT). We demonstrate that few-layer BP systems have a direct-bandgap at *K* point, tunable from 0.955 eV of a monolayer to 0.048 eV of a four-layer sample, and the direct-bandgap decreases exponentially with the increase of the layer number. We also observe that the stacking order has an influence on the stability and band structure of few-layer BP. Furthermore, the bandgap of few-layer BP shows a high sensitivity to the applied E-field. This can be attributed to a giant Stark effect due to the splitting of conduction band (CB) and valence band (VB). What is more, a semiconductor-to-metal transition may occur beyond a critical electric field for four-layer BP, but the direct gap is retaining regardless of the strength of E-field. Our findings show that few-layer BP is a promising candidate for nanoelectronics and optoelectronics applications. It should be noted that this study represents the first attempt in systematically investigating these important electrical properties of few-layer BP by means of vdW-corrected density functional theory (DFT) computations.

2. Computational methodology

All theoretical calculations are based on density functional theory (DFT) implemented in the Dmol^3 package.[19,21] In order to obtain the geometric optimization and the electronic structural of all the structures, we have applied the generalized gradient approximation (GGA) within the Perdew-Burke-Ernzerhof (PBE) exchange correlation functional. The dispersion corrected density functional theory (DFT-D) proposed by Grimme has been employed to describe the long-range van der Waals (vdW) interaction between layers.[3,22] The method is a semiempirical dispersion-correction approach that introduces the correction potential given by the $C_6\ R^{-6}$ term in the DFT formalism.[23] All the atoms in the unit cell are relaxed by a conjugate gradient method until the residual force on each atom is less than 0.005 eV Å^{-1} and the convergence of the total energy is set to 10^{-5} eV. The lattice constant of monolayer boron-phosphide is a = 3.230 Å and b = 3.209 Å in the lowest energy configurations along zigzag direction, with in-plane B-P bond length of 1.853 Å.[24] The 2D Brillouin zone integration is sampled with a 16×16×1 k-point within the Monkhorst-Pack scheme for geometric optimization that is performed under zero electric field and takes a 20×20×1 k-point for electronic structural calculations.[2,3] The vacuum region must be larger than 25 Å in the direction perpendicular to the xy plane in order to avoid the effect of the spurious interaction between neighboring layers. The binding energy of interlayer is calculated as E_n-nE_s. E_n, E_s, and n are the energy of n layer boron-phosphide, single layer boron-phosphide, and layer number, respectively. The effect of E-field on band structure is also taken into account in our study.

3. Results and discussion

To obtain a comprehensive understanding of few-layer BP, we study the atomic and electronic structures of single-layer BP. The geometric parameters of monolayer BP are shown in Figure 1(a), and there are 4 B and 4 P atoms in a unit cell. Simulation results show that monolayer BP is indeed a direct-bandgap semiconductor (as shown in Figure 1(b)) with the bandgap value of 0.955 eV obtained at the K point, which is consistent with previous theoretical data 0.91 eV (VASP) and 0.97 eV (SIESTA).[19,21] We also plot the total DOS and partial DOS projected onto the p state of B and P atoms, as shown in Figure 1(c). It can be seen that the

valence bands from -10 to 0 eV are dominated mainly by p state of P atoms, whereas the conduction bands from 0 to 7.5 eV consist mainly of the p state of B atoms; furthermore, B and P levels contribute nearly the same in higher unoccupied states. When an E-field even up to 0.025 a.u. (1 a.u.=51.36 V/ Å) along the perpendicular direction are applied, no evident effect on the band structure of the single-layer BP is observed.
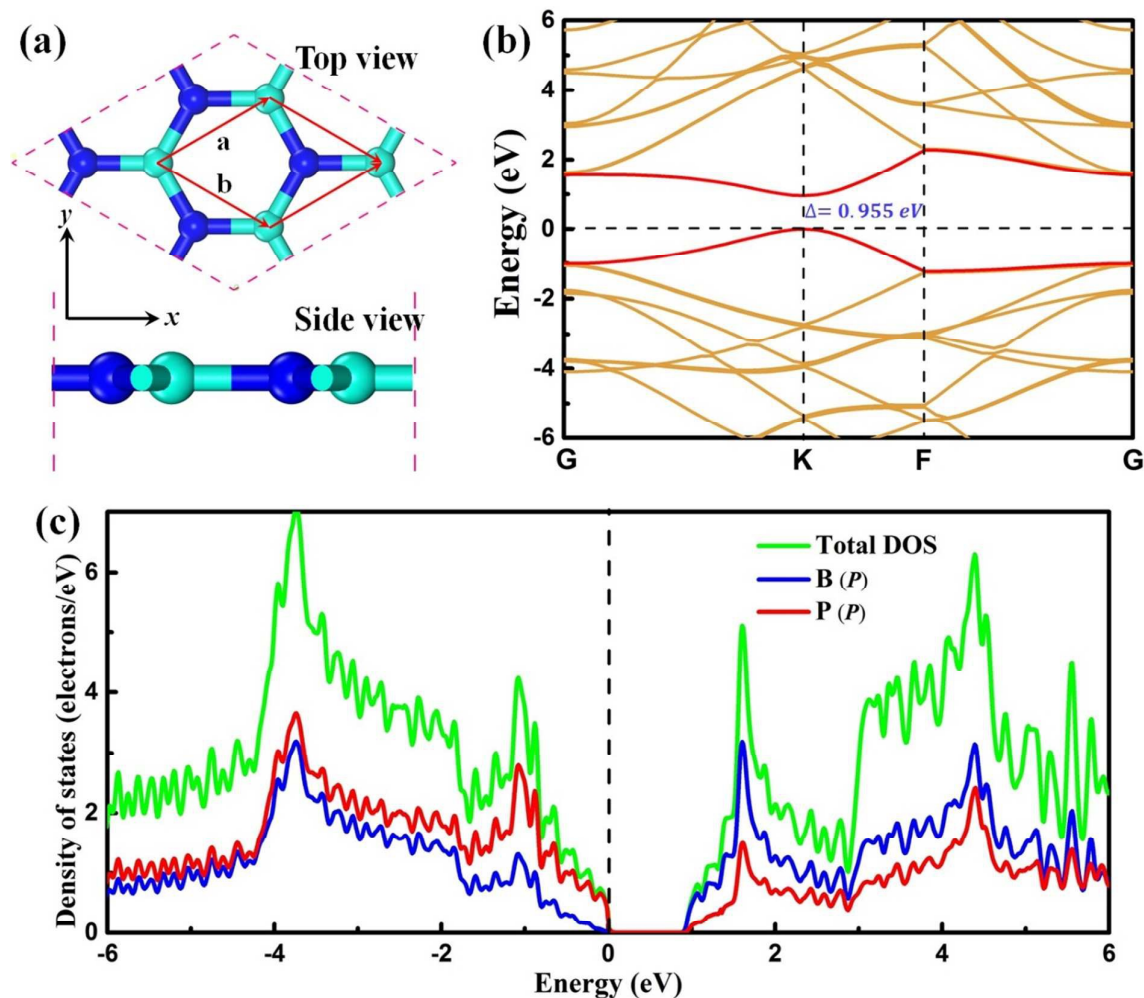

Figure 1. (a) Top and side view of the atomic structure of monolayer BP. The cyan and dark blue balls denote B and P atoms, respectively. The infinite BP plane is parallel to the *xy* plane. (b) and (c) Band structures and total/partial DOS of monolayer, respectively. All of the side views are along the direction of the basis vector *b*.

For bilayer, there are five possible stacking conformations[25], namely, AA-, AAI-, AB-, ABI-, and ABII-stacking (more details in the Supplementary information), respectively. On the basis

of E_{total} and bandgap, AB-stacking is the most favorable configuration among the five possible stacking structures, whereas AA-stacking is the most undesirable one. For AA-stacking (see Figure 2(a)), two BP monolayers are directly stacked without mismatch in the xy plane. However, for AB-stacking (see Figure 2(b)), the center of hexatomic ring that consists of B and P atoms of top layer is positioned at the leftmost B atom of hexatomic ring of bottom layer. In fact, the AB-stacking can be regarded as shifting the top layer of the AA-stacking by the length of B-P bond along x negative direction in the xy plane. The layer-to-layer distances (d-spacing) of AA- and AB-stacking are 3.927 Å and 3.390 Å, respectively. In addition, we find that the total energy of per atom (E_{total}) of AB is ~22 meV lower than that of AA-stacking. We also calculate the band structures of AA- and AB- stacked bilayer BP, as shown in Figure 2(c) and (d), respectively. Although both of the conduction band minimum (CBM) and valence band maximum (VBM) are still located at the K point of AA- and AB-stacking, the stacking orders exhibit significant effect on the direct-bandgap. The AB-stacked bilayer BP possesses a direct-bandgap of 0.746 eV that is much higher than that of AA-stacked bilayer BP (0.230 eV). However, it is worth noting that both of them are smaller than the bandgap value (0.955 eV) of monolayer BP due to the multilayer structure. The data of d-spacing, E_{total}, and bandgap indicate that AB-stacking is the better conformation for bilayer BP.

In order to inquiry what leads to a big difference in d-spacing, E_{total}, and band structure between AA- and AB-stacked bilayer BP, we investigate the charge density difference (CDD) of bilayer BP with different conformations, which is calculated by:

$$\Delta\rho = \rho_{bi} - \rho_1 - \rho_2$$

ρ_{bi}, ρ_1 and ρ_2 are the charge densities of bilayer BP, two isolated monolayer BP, respectively. ρ_1 and ρ_2 are calculated with the atoms in the same unit cell as the atoms in the bilayer BP system. Figure 2(e) gives the charge density difference of AA-stacked bilayer BP, and it is clearly to see that the charge density is redistributed by forming electron-rich and hole-rich regions in the interlayer space, as observed previously.[26-28] The charge is accumulated on the B atoms, while it is dissipated on the P atoms and in the interlayer region. However, there is no charge transfer in the AA-stacking according to the Mulliken charge transfer calculation, which means that the electrical neutrality of each constituent is kept. The analysis indicates that charge density redistribution is mainly ascribed to the electrostatic repulsion as

demonstrated in the silicone/GaS and graphene/BN heterosheets.[27,29] By contrast, the AB-stacking shows a slightly different behaviour, with the distribution of charge accumulation and dissipation (see Figure 2(f)). On the bottom, B atoms accumulate charges in the z direction and slightly dissipate charges in the AB-stacking bilayer BP plane, while P atoms dissipate charges in the z direction. On the top, the charge is dissipated on the B atoms, while is accumulated on the P atoms. In the case of AB-stacking, a strong charge transfer is found from the bottom layer to the top layer, and the ranges of charge redistributions is much wider as compared to the AA-stacking. The charge transfer Q calculated by Mulliken charge analysis is -0.05 e that indicates a weak vdW interaction is presented between two layers.[27,30] Based on the aforementioned results, we propose that the AB-stacked conformation is more stable than AA-stacking for bilayer BP system. Additionally, the splitting of the conduction band and valence band induced by the interlayer coupling, results in the decrease in the bandgaps of bilayer BP as compared with that of monolayer BP.[10]
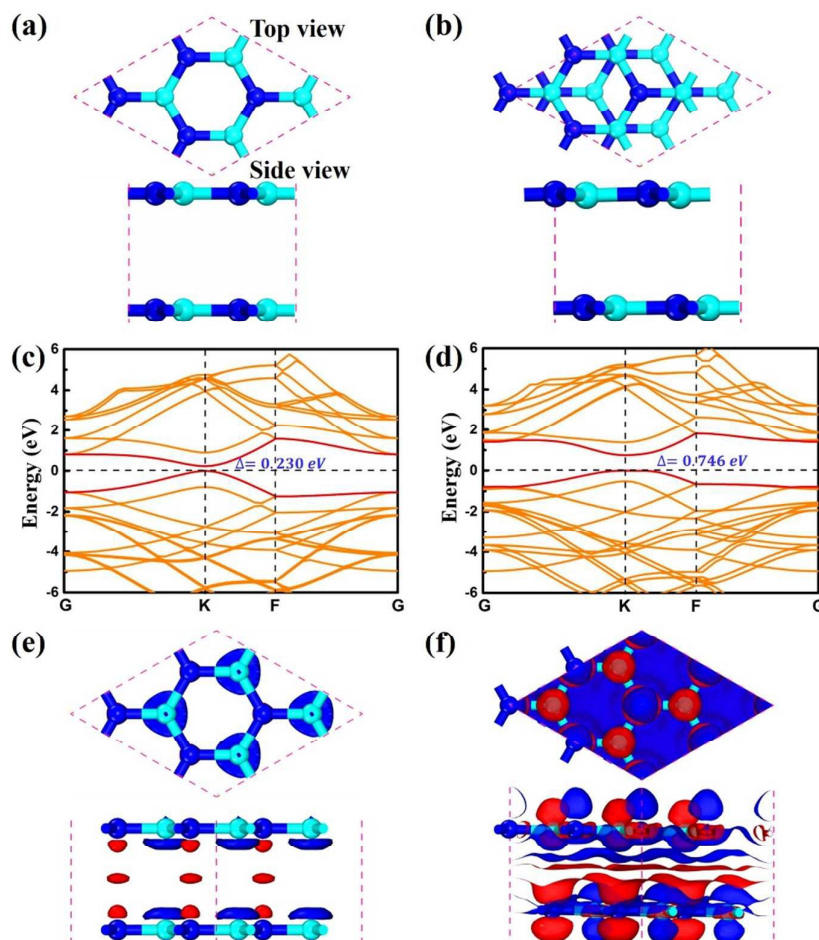
Figure 2. Geometric and electronic properties of AA- and AB-stacked bilayer BP: (a) and (b) top and side views of atomic structure; (c) and (d) band structures; (e) and (f) top and side views of charge density difference. The red and blue represent charge depletion and accumulation, respectively, where the isosurfaces refer isovalues of 0.001 e/Å^3.

For trilayer BP, ten kinds of stacking are considered in this work (more details in the Supplementary information). In the case of ABC-stacking, the character C implies the top BP layer with a shift is relative to the bottom BP layer by two bonds of B-P along x negative direction. There is a surprising difference between bandgap values and the bandgap decreases in the order: AAAI-stacking $(0.845$ eV$)$ **>** ABA-stacking $(0.722$ eV$)$ **>** ABAIII-stacking $(0.621$ eV$)$ **>** ABC-stacking $(0.592$ eV$)$ **>** AABI-stacking $(0.523$ eV$)$ **>** AAAII-stacking $(0.5$ eV$)$ **>** AAB-stacking $(0.314$ eV$)$ **>** AAA-stacking $(0.081$ eV$)$ **>** ABAII-stacking $(0.02$ eV$)$ **>** ABAI-stacking $(0.018$ eV$)$. From PBE calculations, we find that the values of E_{total} of ABA- and ABC-stacking are very close, and both of them are ~45 meV lower than that of AAA-stacking; moreover, their structure are respectively shown in Figure 3 (a)-(c). Considering the two key factors of bandgap and E_{total}, we suggest that ABA- and ABC-stacking are favorable conformations for trilayer BP. The band structures of the three stacked conformations are calculated and illustrated in Figure 3(d)-(f), respectively. ABA-stacked trilayer possesses the widest bandgap of 0.722 eV, while the bandgap of ABC- and AAA-stacked trilayer are 0.592 eV and 0.081 eV, respectively. It is clear to see that both of CBMs and VBMs for AAA- and ABC-stacking are still located at the K point, which means their bandgaps belong to the direct-bandgap. On the contrary, VBM of ABA-stacking is located between K and F point, which indicates ABA-stacking has an indirect-bandgap. Compared with bilayer BP, the splitting of the valence band and conduction band of trilayer BP is more remarkable. From the viewpoint of bandgap, ABC-stacking is the best conformation for trilayer BP due to the direct-bandgap.

In order to further explore what causes the above difference in E_{total} and electronics, we also analyse the charge density difference of AAA-, ABA-, and ABC-stacking trilayer BP. The

CDDs for these three stacked structures are shown in Figure 3 (g)-(i), respectively. As we can see, the charge density is redistributed by forming electron-rich and hole-rich regions within all layers. For the ABA-stacking, the charge redistribution of the top and bottom layer is almost the same duo to the similar interlayer interaction deriving from the intermediate layer. The majority of charge is accumulated on the intermediate layer and partly on the vicinity of surface B atoms, while charge is depleted on the P and B atoms. On the contrary, for ABC-stacking, the charge redistribution is different among each BP layer. The charge depletion of the top layer is evidently less than that of bottom layer, which indicates that a strong charge transfer is from other layers to top layer. The charge depletion and accumulation respectively occur on the upper and lower surface of intermediate layer. Besides, the charge redistributions of ABA- and ABC-stacking are more obvious than that of AAA-stacking, which results from the relatively stronger interaction between the adjacent layers. The formation of the electron-hole regions is attributable to the interlayer interaction and stacking order, which drives the interlayer charge transfer from one layer to another.[3,26,31] According the Mulliken charge analysis, we can find that the intermediate layer in AAA- and ABA-stacking obtains 0.008 and 0.112 e from the adjacent layers, respectively, while the charge transfer is 0.02 and 0.04 e from the bottom layer to the intermediate layer and to top layer in the ABC-stacking respectively. This suggests that stacking order has also significant effect on the charge transfer.[26,32]
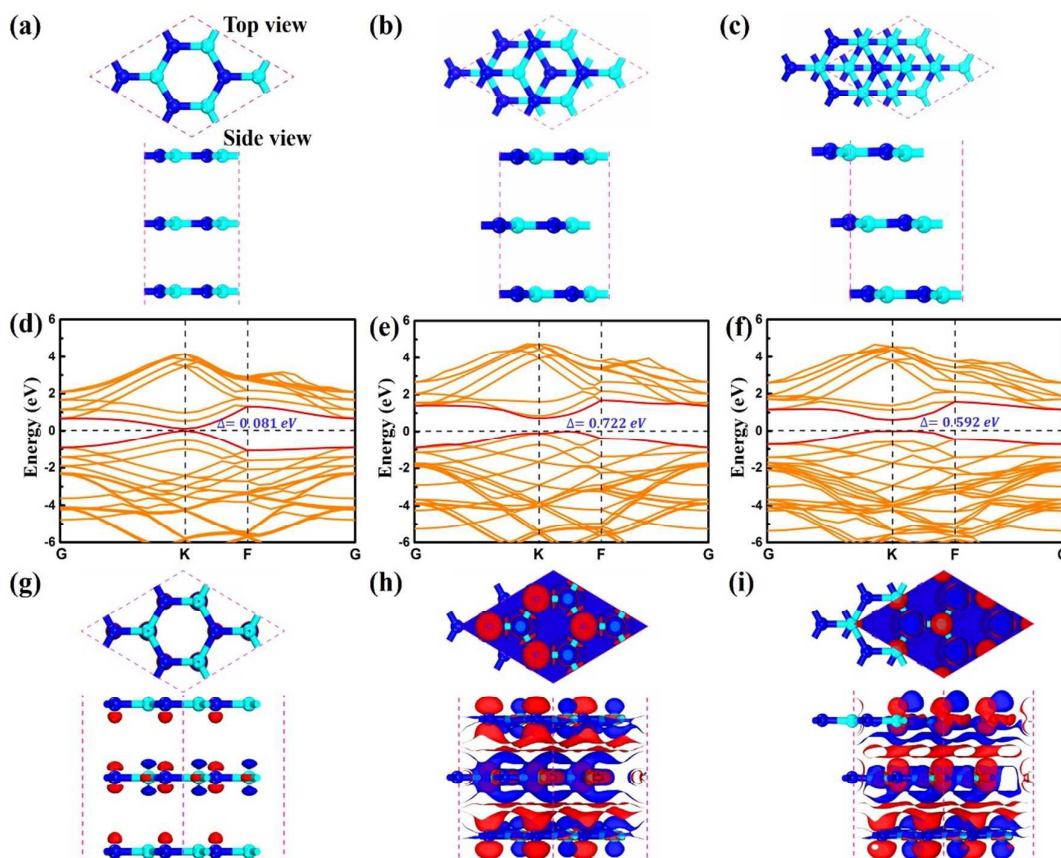
Figure 3. Three stacking structure of trilayer BP. Top and side view of atomic structure (a) AAA-stacking, (b) ABA-stacking, and (c) ABC-stacking. Band structures of (d) AAA-stacking, (e) ABA-stacking, and (f) ABC-stacking. The charge density difference (g) AAA-stacking, (h) ABA-stacking, and (i) ABC-stacking. The red and blue represent charge depletion and accumulation, respectively, where the isosurfaces refer isovalues of 0.001 e/Å^3.

According to the results of trilayer BP, ABAB- and ABCA-stacking are considered for four-layer BP. ABCA-stacked four-layer BP possesses the direct-bandgap of 0.467 eV, while ABAB-stacked four-layer BP has indirect-bandgap of 0.628 eV. The band structures of four-layer BP have similar characteristic of splitting of the CBs and VBs with the bilayer and trilayer due to interlayer interaction with the further decrease in bandgap. In order to have a good overview, the lattice constants (a, b), bond length (l), d-spacing, ΔE_{total}, charge transfer (Δq), and bandgap of BP from monolayer to four-layer have been calculated (see Table 1). Although the lattice constant (a, b) undergoes a slight change from monolayer to few-layer, the values of the lattice constants (a, b) are almost the same in all the few-layer BP. On the

other hand, the bond length is also very similar. It is worth noticing that the values of d-spacing, ΔE_{total}, charge transfer (Δq), and bandgap in AB-stacking BP are a little higher than that of ABC-stacking BP when $n > 2$. The ΔE_{total} increases by 27.77 meV from the bilayer to the four-layered, which suggests that the vdW interaction enhance with the increase of layer number. It is also noticeable that the bandgap decreases with the increasing of layer number or with the decreasing of d-spacing. The interesting thing is that ABC-stacking BP has a direct-bandgap, while ABA-stacking BP has an indirect-bandgap when $n > 2$.

Table 1 Calculated lattice constants a and b, bond length (l) of B-P Δd, charge transfer Δc, and binding energies (ΔE) of n-layer BP

n	Stacking order	a (Å)	b (Å)	l (Å)	d-spacing	ΔE (meV/atom)	Δq (e)	Bandgap (eV)
1	A	3.230	3.209	1.853				0.955
2	AB	3.213	3.211	1.856	3.390	133.96	0.051	0.746
3	ABA	3.212	3.211	1.854	3.400	152.49	0.112	0.722 indirect-bandgap
3	ABC	3.212	3.211	1.855	3.365	151.69	0.060	0.592
4	ABAB	3.212	3.211	1.854	3.390	161.73	0.132	0.628 indirect-bandgap
4	ABCA	3.212	3.211	1.854	3.362	161.02	0.056	0.467

Generally, the PBE method underestimates bandgap. As a result, in order to check the bandgap of the most stable few-layer BP, we employ the HSE06 hybrid functional calculations.[33] The results comparing HSE06 and PBE calculations indicate that the PBE bandgaps are underestimated by

0.27-0.414 eV for few-layer BP materials. In addition, the bandgap of few-layer BP computed with HSE06 decreases monotonically with the increasing of layer number, varying from 1.369 eV for monolayer to 0.737 eV for four-layer.

A large number of theoretical and experimental studies have indicated that the E-field can effectively tune the band structure of materials, especially the bandgap of the two dimensional materials.[11,20,34-36] Thus, it is interesting to investigate the tunable mechanism of the vertical E-field as to the band structure of few-layer BP. In our study, we examine the BP materials from monolayer to four-layer. The out-plane electric field applied is perpendicular to the few-layer BP slab, and the values from -0.006 to 0.006 a.u. are used except for the ABA-stacking which is from 0 to 0.012 a.u.. The positive direction of the E-field is from the bottom layer to the top layer, as shown in Figure 4. In the case of monolayer BP, its bandgap is almost unchanged with the increasing of E-field along the positive and negative direction due to its planar structure. Contrary to that, the bandgaps of AB-stacked bilayer BP and ABC-stacked trilayer BP show a monotonically increasing relationship within the range of -0.006 to 0.006 a.u. and -0.003 to 0.003 a.u.(see Figure 4(b) and (d)). For the ABA-stacking, the impact of positive and negative E-field on the bandgap of ABA-stacking is the same due to the high symmetry of the z direction. As shown in Figure 4(c), the variation of bandgaps of the ABA-stacking with the E-field exhibits an approximately proportional relationship, which can be retained up to 0.24 a.u. or higher. This indicates that the ABA-stacking possesses a larger tunable region compared with AB- and ABC-stacked structure. The variation trend of bandgap of bilayer and trilayer is opposite to that of MoS_2, phosphorene, and blue phosphorus with the changes of E-field.[11,21,34,37] Although the tunable region of bandgap of few-layer BP is smaller than that of MoS_2, phosphorene, and blue phosphorus, the bandgap of few-layer BP is more sensitive to E-field. As a result, few-layer BP possesses the strong regulating capacity on band structure under low E-field. For ABAB-stacking, the bandgap closes up and a semiconductor-to-metal transition occurs as the electric field of -0.002 and 0.004 a.u. are applied, but as the electric field is -0.003 and 0.002 a.u. as illustrated in Figure 4(e) and (f). The binding energies of all stacking orders of layer BP indicate that interaction between the adjacent layers can be enhanced by applying appropriate electric field. It is to be seen that the bandgaps can be tuned significantly by a small external E-field. In addition, the lattice constants and bond length of few-layer BP under various E-field are the same as the values (without E-field) shown in Table 1. So geometrical structures of few-layer BP are not affected by external E-field. In

order to further understand this mechanism, we investigate the band structures of few-layer BP under different electric fields and analyse contributions of each layer to all bands near the Fermi level. Under the case without electric field, the CBs and VBs of few-layer BP have been split due to the interlayer coupling as discussed before. The splitting will be further enhanced and the splitting bands are redistributed to every layer under the electric field, as shown in Figure 5(a). The splitting of CBs and VBs enhances with the increasing of electric field, resulting in the further reduction of bandgap or even eventually vanishing at a critical field intensity (Figure 5(a)).[37,39] Here the difference of electrostatic potential caused by breaking the symmetry of few-layer BP results in the shifting down of CBs of different layers, as depicted in Figure 5(b).[38,40] The bandgap modulation of few-layer BP under the E-field can be attributed to the giant Stark effect which has been observed in boron nitride nanotubes, black phosphorus, bilayer MoS_2, and boron nitride nanoribbons.[3,21,38,41,42] Moreover, the energy difference of the CBs and VBs depends on the electrostatic potential difference between the top and bottom layers under the E-field. Hence few-layer BP with more layers has a more sensitive response of the bandgap to the electric field, which suggest that four-layer BP can be turned into metal by an available E-field. So increasing the layer number is a feasible scheme to realize the transformation of semiconductor to metal in 2D materials under high E-field. It is also noted that four-layer BP, the variation of the bandgaps, is an approximately symmetric parabolic curve within the specified electric field (Figure 4(e) and (f)). The nonlinear variation under lower E-field can be owed to the spatial charge separation which is more significant for the thicker cases as they possess more hybrid states from the CB or VB with larger splitting energies. The CB shifts toward the Fermi level under the higher E-field, which means the semiconductor material may become a metal with an enhanced charge screening effect, and shows another nonlinear relationship between the bandgap and E-field.
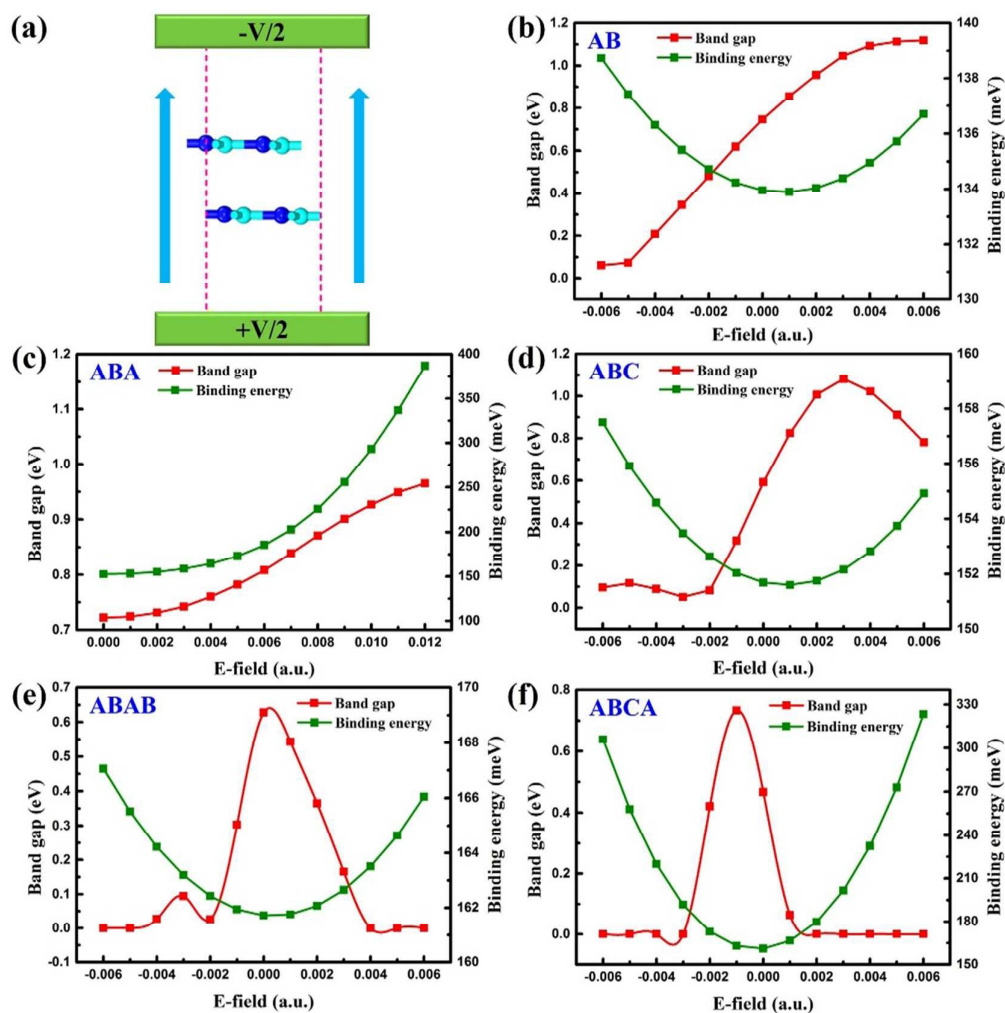
Figure 4. (a) The directions of the electric field. (b)-(f) Band gaps and binding energies of different stacked structures as a function of the electric field.
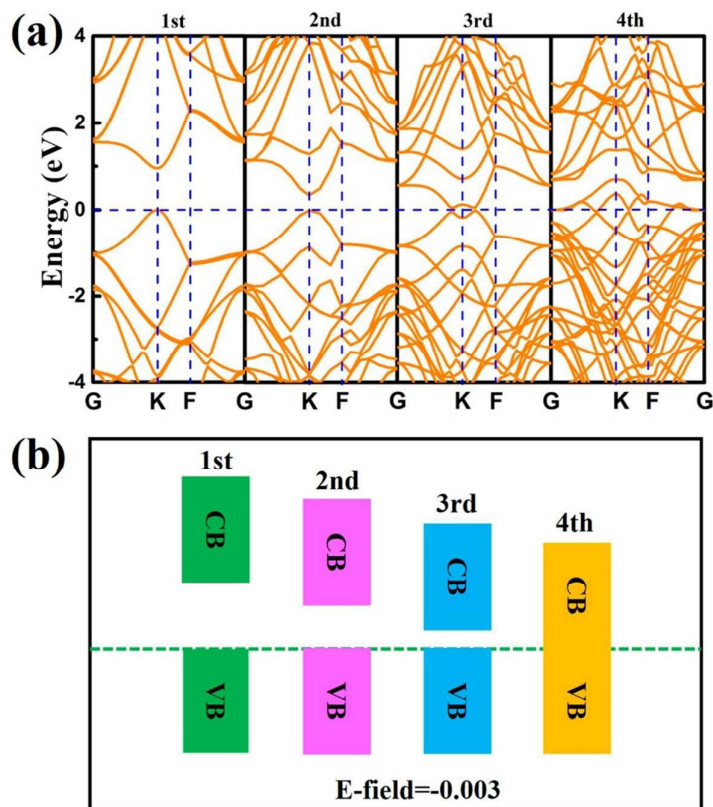
Figure 5. (a) Calculated band structures of few-layer BP under the electric field of -0.003 a.u.. (b) A schematic view of the bands shifting for four-layer BP under the electric field of -0.003 a.u.. The Fermi level is set to zero and marked by green dotted lines.

The mechanism can also be understood by investigating the charge redistribution under the E-field. The charge can be transferred from one layer to another duo to the interlayer interaction, which suggests that the difference in the chemical environment between two adjacent layers can be affected by modulating charge transfer.[3,40] In order to further validate the results discussed above, we investigate the charge density distribution of the AB-stacked bilayer BP under different electric fields, namely -0.003, -0.006, 0.003 and 0.006 a.u.. Figure 6 shows the charge density difference of AB-stacking with various E-fields. As can be seen, charges accumulate on the positive potential layer BP, while they deplete at the negative potential layer BP. More charge accumulation and depletion can be observed at each layer BP of the AB-stacking with the increased electric field, further narrow or broaden the bandgap. Furthermore, the charge is significantly accumulated on the P atoms and depleted on the B atoms in the interlayer space between the top layer and the bottom layer with the electric field

increasing along positive direction. Furthermore, the in-plane bottom layer occurs slight depletion, which is contrary to the case along negative direction. The results demonstrate that the E-field is an effective way to rearrange charges and modulate chemical environment, thus the bandgap can be tuned regularly by applying a reasonable E-field.
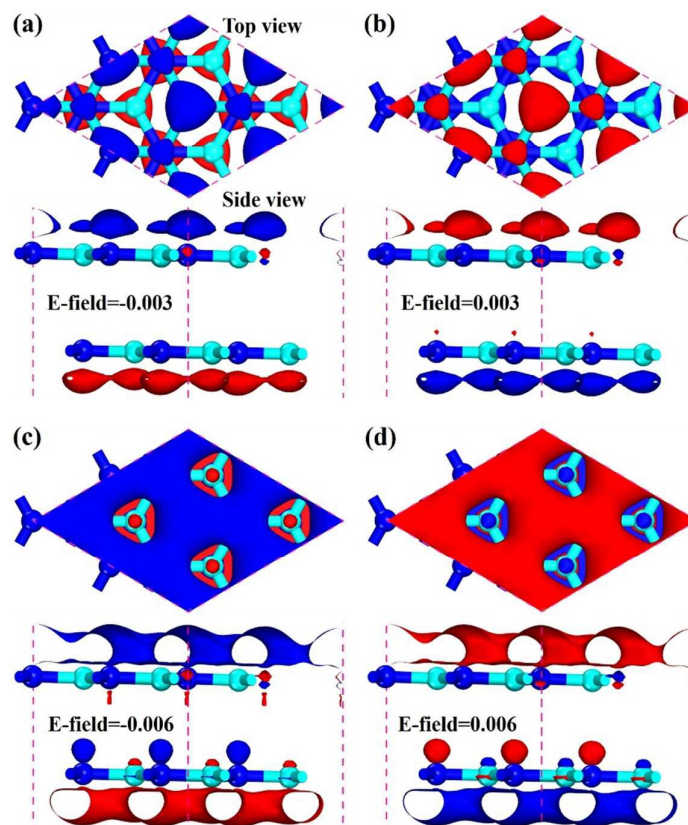

Figure 6. (a)-(d) The charge density distribution of the AB-stacking under electric field of -0.003, -0.006, 0.003 and 0.006 a.u., respectively. The red and blue represent charge depletion and accumulation, respectively, where the isosurfaces refer isovalues of 0.001 e/Å^3.

Conclusions

In summary, by means of DFT computations, we perform a theoretical investigation to study structural and electrical properties of few-layer BP. We also demonstrate that AB-stacking is most stable conformation for bilayer and ABA- and ABC-stacking are favoured in the case of trilayer BP. Nevertheless, for four-layer BP, the stable conformations are ABAB- and ABCA-stacking. We also show that both of the monolayer BP and AB-stacking bilayer BP

possess a direct-bandgap. At $n > 2$, the direct-bandgap feature can be retained in the ABC-stacking structural models, while ABA-stacking BP systems possess an indirect-bandgap. According the charge density difference, it reveals that different stacking orders and layer number may affect the bands splitting of each layer. Moreover, the bandgap has a decreased monotonically relationship with the increased layer number, and the stacking order can influence the direct-bandgap or indirect-bandgap behavior of few-layer BP. Typically, an increase of the electric field along negative direction within the available range decreases the bandgap of bilayer and trilayer, which is contrary to the positive E-field. For four-layer BP, a semiconductor-to-metal transition may occur beyond a critical electric field, and its bandgap is always directly independent of the strength of the external E-field (-0.006 a.u. $< E <$ 0.006 a.u.). The tunable mechanism of bandgaps under the vertical electric field can be governed by a giant Stark effect, and further demonstrated by the charge density distribution of different E-field. Our findings motivate more efforts in developing new 2D material systems using band structure engineering, and may light up new opportunities in fabricating new electronics and opto-electronics devices based on few-layer BP.

Acknowledgements

Notes and references

1.   L. Kou, T. Frauenheim and C. Chen, *The Journal of Physical Chemistry Letters*, 2014, **5**, 2675-2681.
2.   X. Sui, C. Si, B. Shao, X. Zou, J. Wu, B.-L. Gu and W. Duan, *The Journal of Physical Chemistry C*, 2015, **119**, 10059-10063.

3.   X. Li, Y. Dai, Y. Ma, S. Han and B. Huang, *Physical Chemistry Chemical Physics*, 2014, **16**, 4230-4235.
4.   L. Li, Y. Yu, G. J. Ye, Q. Ge, X. Ou, H. Wu, D. Feng, X. H. Chen and Y. Zhang, *Nature nanotechnology*, 2014, **9**, 372-377.
5.   S. Balendhran, S. Walia, H. Nili, S. Sriram and M. Bhaskaran, *small*, 2015, **11**, 640-652.
6.   S. Kim, A. Konar, W.-S. Hwang, J. H. Lee, J. Lee, J. Yang, C. Jung, H. Kim, J.-B. Yoo and J.-Y. Choi, *Nature communications*, 2012, **3**, 1011.
7.   B. Radisavljevic, A. Radenovic, J. Brivio, V. Giacometti and A. Kis, *Nature nanotechnology*, 2011, **6**, 147-150.
8.   J. Qiao, X. Kong, Z.-X. Hu, F. Yang and W. Ji, *Nature communications*, 2014, **5**.
9.   S. Appalakondaiah, G. Vaitheeswaran, S. Lebegue, N. E. Christensen and A. Svane, *Physical Review B*, 2012, **86**, 035105.
10.   Y. Cai, G. Zhang and Y.-W. Zhang, *Scientific reports*, 2014, **4**.
11.   Y. Li, S. Yang and J. Li, *The Journal of Physical Chemistry C*, 2014, **118**, 23970-23976.
12.   S. P. Koenig, R. A. Doganov, H. Schmidt, A. C. Neto and B. Oezyilmaz, *Applied Physics Letters*, 2014, **104**, 103106.
13.   X. Han, H. Morgan Stewart, S. A. Shevlin, C. R. A. Catlow and Z. X. Guo, *Nano letters*, 2014, **14**, 4607-4614.
14.   E. S. Reich, *Nature*, 2014, **506**, 19.
15.   M. Buscema, D. J. Groenendijk, S. I. Blanter, G. A. Steele, H. S. van der Zant and A. Castellanos-Gomez, *Nano letters*, 2014, **14**, 3347-3352.
16.   J. Dai and X. C. Zeng, *The Journal of Physical Chemistry Letters*, 2014, **5**, 1289-1293.
17.   H. Liu, A. T. Neal, Z. Zhu, Z. Luo, X. Xu, D. Tománek and P. D. Ye, *ACS nano*, 2014, **8**, 4033-4041.
18.   H. Şahin, S. Cahangirov, M. Topsakal, E. Bekaroglu, E. Akturk, R. T. Senger and S. Ciraci, *Physical Review B*, 2009, **80**, 155453.
19.   D. Çakır, D. Kecik, H. Sahin, E. Durgun and F. M. Peeters, *Physical Chemistry Chemical Physics*, 2015, **17**, 13013-13020.
20.   T. Chu, H. Ilatikhameneh, G. Klimeck, R. Rahman and Z. Chen, *Nano letters*, 2015, **15**, 8000-8007.
21.   Q. Liu, L. Li, Y. Li, Z. Gao, Z. Chen and J. Lu, *The Journal of Physical Chemistry C*, 2012, 116, 21556-21562.
22.   D. C. Sorescu and B. M. Rice, *The Journal of Physical Chemistry C*, 2010, **114**, 6734-6748.
23.   S. Grimme, *Journal of computational chemistry*, 2006, **27**, 1787-1799.
24.   Y. Cai, Q. Ke, G. Zhang and Y.-W. Zhang, *The Journal of Physical Chemistry C*, 2015, **119**, 3102-3110.
25.   D. W. Xu, H. Y. He, R. Pandey and S. P. Karna, *Journal of Physics: Condensed Matter*, 2013, 25, 345302.
26.   Y. Ma, Y. Dai, M. Guo and B. Huang, *Physical Review B*, 2012, **85**, 235448.

27. Y. Ding and Y. Wang, *Applied Physics Letters*, 2013, **103**, 043114.
28. J. Martin, N. Akerman, G. Ulbricht, T. Lohmann, J. Smet, K. Von Klitzing and A. Yacoby, *Nature Physics*, 2008, **4**, 144-148.
29. E. Kan, H. Ren, F. Wu, Z. Li, R. Lu, C. Xiao, K. Deng and J. Yang, *The Journal of Physical Chemistry C*, 2012, **116**, 3142-3146.
30. W. Geng, X. Zhao, H. Liu and X. Yao, *The Journal of Physical Chemistry C*, 2013, **117**, 10536-10544.
31. W. Hu, Z. Li and J. Yang, *The Journal of chemical physics*, 2013, **138**, 124706.
32. X. Li, S. Wu, S. Zhou and Z. Zhu, *Nanoscale research letters*, 2014, **9**, 1-9.
33. Z. K. Tang, X. B. Li, D. Y. Zhang, Y. N. Zhang and L. M. Liu, *Journal of Materials Chemistry C*, 2015, 3(13): 3189-3197.
34. B. Ghosh, S. Nahas, S. Bhowmick and A. Agarwal, *Physical Review B*, 2015, **91**, 115433.
35. X. Liu and Z. Li, *The Journal of Physical Chemistry Letters*, 2015, **6**, 3269-3275.
36. L. Huang, N. Huo, Y. Li, H. Chen, J. Yang, Z. Wei, J. Li and S.-S. Li, *The journal of physical chemistry letters*, 2015, **6**, 2483-2488
37. T. F. Cao, X. B. Li, L. M. Liu and J. J. Zhao, *Computational Materials Science,* 2016, 112, 297-303.
38. Q. Wu, L. Shen, M. Yang, Y. Cai, Z. Huang and Y. P. Feng, *Physical Review B*, 2015, **92**, 035436.
38. K. Dolui, C. D. Pemmaraju and S. Sanvito, *Acs Nano*, 2012, **6**, 4823-4834.
40. S.-s. Li, C.-w. Zhang, W.-x. Ji, F. Li and P.-j. Wang, *Physical Chemistry Chemical Physics*, 2014, **16**, 22861-22866.
41. T. Wang, Y. Liu, Q. Guo, B. Zhang, K. Sheng, C. Li and Y. Yin, *Journal of the Korean Physical Society*, 2015, **66**, 1031-1034.
42. A. Chaves, T. Low, P. Avouris, D. Çakır and F. Peeters, *Physical Review B*, 2015, **91**, 155311.